SVENSKA GEOFYSISKA FÖRENINGEN

VOLUME 10, NUMBER 3 Tellus AUGUST 1958

A QUARTERLY JOURNAL OF GEOPHYSICS

Comparative Studies of 500 mb Barotropic Forecasts Based on Different Analyses

By ROY BERGGREN, Swedish Meteorological and Hydrological Institute, Stockholm

(Manuscript received October 2, 1957)

Abstract

Some barotropic 500 mb forecasts are compared in the following manners:
1) comparison of the differences between forecasts made from analyses with identical boundary regions but different inner parts
2) comparison of forecasts made from two independent analyses based on identical material, and
3) comparison between forecasts based on two analyses with identical inner region but different boundary regions.

The result of a computation of the standard deviation of the vorticity and the Jacobian $J(\eta, \phi)$ is given and discussed, the deviation being due entirely to the personal factor in upper air analysis.

Introduction

When discussing numerical forecasts such as barotropic 500 mb forecasts one has a definite need of some kind of verification figures. The ones mostly used in the past have been the correlation coefficient between observed and forecast height changes, the root-mean-square difference of these values and so on. In an earlier paper (1957, in the following called paper I) the author reported the result of an experiment in which the initial 500 mb chart as well as the barotropic 24h and 48h forecasts were kept constant, while different verification analyses were used. Thus, the forecast height changes were the same all through the experiment, while the observed changes varied with the different verification analyses. The latter analyses were based on identical observation material and the reported deviations were entirely due to the personal factor in upper air analysis.

In this paper another experiment will be discussed, in which the verification charts are the same all the time while the initial charts vary, the variation being entirely due to the method of analysis. The observation material was identical for all the four different analyses used for the experiment. Thus, the observed changes varied this time with the initial analysis as did the forecast changes.

The 500 mb forecasts were performed as discussed in papers by Staff Members, Dept. of Met., Univ. of Stockholm (1954) and Bolin (1955). The grid size was about 300 km and the area used is indicated in fig. 1. The total forecast area was about 12,000 km × 9,000 km and the verification was performed over an area of 8,000 km × 4,000 km (see fig. 1).

Among the 29 analyses discussed in paper I three were picked out. The first one was the author's analysis (from here on called analysis

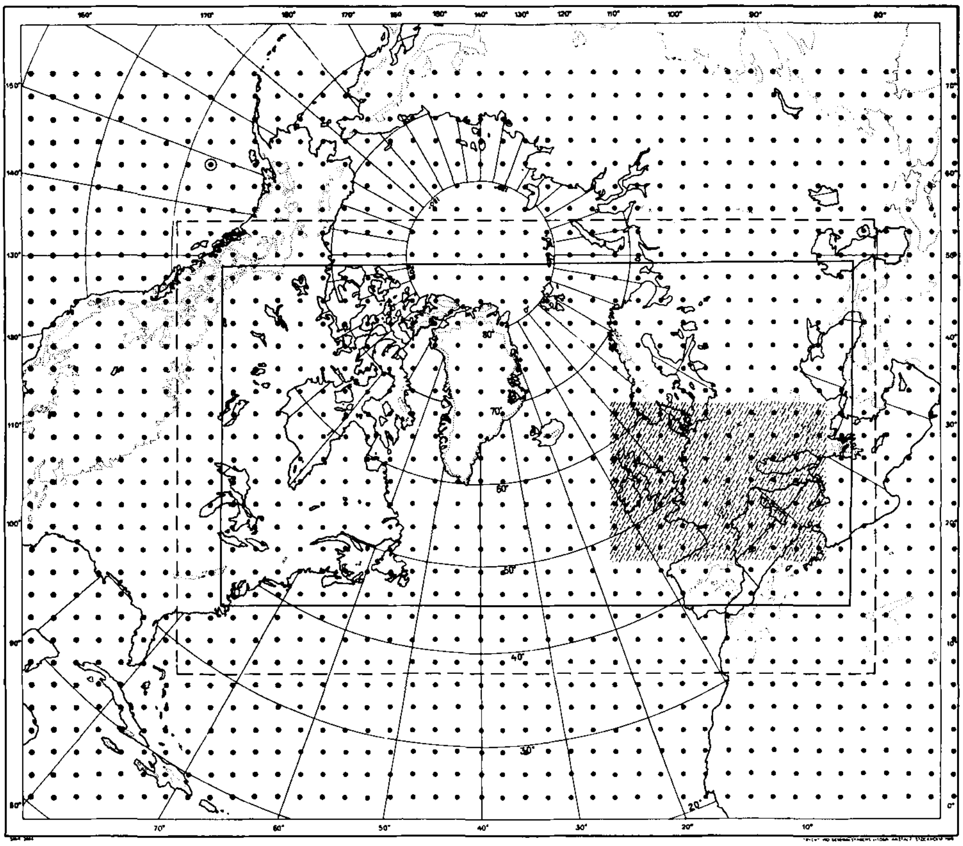

Fig. 1. Location of the grid used in the numerical forecasts. The solid line indicates the region within which verification was made. The dashed line gives the boundary outside which the analyses discussed in paragraph 1 were identical. The calculations discussed in paragraph 5 were performed over the small region with the dash-dotted lines.

A) which gave a low value for the correlation coefficient for the 24h forecast. The second one (analysis B) was the analysis that gave the highest 24h correlation coefficient and as the third analysis a numerical analysis was chosen (analysis C). The numerical analysis was used already in paper I and was constructed according to the scheme laid down by BERGTHORSON and DÖÖS (1955) and by DÖÖS and EATON (1957).

In the earlier experiment the analysis was restricted to a region slightly larger than the verification area indicated in fig. 1. Thus, it was necessary to increase the analysis area of analyses B and C. This was done in such a way that the boundary region from analysis A was fitted to the inner part of analyses B and C. In fig. 1 is indicated the boundary outside which the three analyses were identical.

Furthermore, the analyst who once performed analysis B completed his analysis to the outer boundary of fig. 1 (analysis B^1). Thus, the author had at his disposal four analyses that were to be brought together and compared in three different ways:

1) Comparison of the differences between forecasts made from analyses with identical boundary regions but different inner parts, (analyses A, B and C),

2) comparison of forecasts made from two independent analyses based on identical material (analyses A and B^1), and

3) comparison between forecasts based on two analyses with identical inner region but different boundary regions (analyses B and B^1).

Before going into numerical details two things must be stressed:

a) this discussion deals only with one

Table I. The standard deviation of the difference between analyses A, B, B[1] and C and the corresponding forecasts. The computations were made over the inner area given in fig. 1, consisting of 420 grid points.

Analysis pairs	A—B	B—C	A—C	A—B[1]	B[1]—C	B—B[1]
Analysis	26 gdm	24	31	26	24	0
24h forecasts	29	33	31	30	33	9
48h	54	41	30	56	50	39

single case and it is not claimed that general conclusions can be drawn from it. The goal of this paper is only to show what may happen under certain conditions,

b) the case studied in this paper and in paper I represents a simple case from the analyst's point of view. The observed differences in analysis are therefore relatively small.

Let us first examine numerical estimates of the differences between the analyses used during the experiment. As a measure of the deviations between the analyses the author has used the standard deviation (d) of the difference between the height values at the 420 grid points of the verification area indicated in fig. 1.

In the literature on numerical analysis the root-mean-square difference (RMS) is sometimes given.

The difference between d and RMS is small when $(\bar{A}-\bar{B})$ is a small quantity ($\bar{A}$ and $\bar{B}$ being the mean value of the height of the 500 mb surface over the area considered) as is always the case when we compare different analyses over a relatively large area. The reason for using d in this paper is the fact that the same quantity is calculated for the different forecasts and in these the differences $(\bar{A}-\bar{B})$ may reach very large values (in one case 148 geodynamic meters (gdm)).

In table I the values of d are given and they ought to be compared with those given by earlier authors. CRESSMAN and GILCHRIST (1954) have given the values in table II. They used three different analyses together with a numerical one. The two first analyses (1 and 2) "were prepared very carefully by experienced analysts who took all the time they needed for their completion. Analysis 3 was made hurriedly under operational conditions."

Cressman and Gilchrist made the computation over a grid of 19 × 19 points or approximately 5,400 × 5,400 km. From this grid 222 points were selected "as being those where sufficient data were available to permit a fair comparison". Thus, the number of points involved was only slightly more than half that used in this paper. Furthermore, the investigated area was to a large extent situated over the North-American continent in the former case while the one used in this paper covers wide parts of the northern part of the Atlantic Ocean. It is therefore reasonable to get larger d-values in the latter case.

Table II. The standard deviation of the difference between three conventional analyses (1, 2 and 3) and a numerical one (0) as given by Cressman and Gilchrist (1953).

Analysis pairs	1—2	1—3	2—3	0—1	0—2	0—3
d	15 gdm	20	18	21	22	21

Table III. The root-mean-square difference between two conventional routine analyses (C_1 and C_2) and one numerical analysis (N). The values within brackets represent values for a small area with a dense net work of observing stations. Bergthorson and Döös (1955).

Analysis pairs	N—C_1	N—C_2	C_1—C_2
7 cases (12h forecast)	26 (21) m	24 (18)	26 (20)
2 cases (24h forecast)	43 (29)	49 (33)	36 (28)

If we now compare the values given by BERGTHORSON and DÖÖS (1954) (table III) with those in table I we find that the mean value for seven cases is about the same as the ones given in table I. A smaller area (3 000 km × 2 400 km) gave values 5–6 m lower. In the seven cases a 12h forecast was used as a first approximation. The numerical analysis discussed in this paper, however, was based on a 24h forecast. For that reason we ought to compare the values for the two cases that included a 24h forecast. From these values we can see that the values given in table I are lower than the ones in table III. This is in agreement with the above-mentioned fact that the case studied in this paper represents a simple case from the analyst's point of view.

The mean value of the root-mean-square difference given by Döös and EATON (1957) was 34 m and was based on a five month trial period (about 125 cases) during which the numerical analysis technique was used on a routine basis. The investigated area was the northern part of the Atlantic Ocean between 25° N and 65° N, i.e. an area with a scanty net work.

1. *Comparison between forecasts based on analyses with identical boundary regions*

In fig. 2 are given all analyses and forecasts discussed in the three first paragraphs of this paper. The upper row contains four different versions of the 500 mb pattern for 7 November 1949, 0300 GMT. The boundary regions of the three analyses A, B and C are identical and in addition to these analyses, analysis B^1 is indicated in fig. 2 b with dashed lines. The verification charts for 8 and 9 November 1949, 0300 GMT are given in figs. 2 g and k, respectively. Figs. 2 d–f and 2 h–j give the 24h and 48h forecasts, respectively, placed below the corresponding initial chart. The forecasts based on analysis B^1 are given by dashed lines on the forecasts based on analysis B.

As can be seen at a first rapid visual inspection of the forecast charts they all contain the same main error, viz. the trough over Central Europe and the Mediterranean is forecast to move too far to the northeast. Furthermore, the cyclogenesis over the Atlantic east of Newfoundland was missed by all forecasts. Over she westernmost part of the verification area the forecasts show better agreement with the verification charts. On the whole the difference between the forecasts are rather small.

On the forecast charts in fig. 2 d, f, h, and j are also indicated the errors in the forecast, given as the difference between the forecast chart and the verification chart. Thus, a minus-sign on fig. 2 indicates a region in which the forecast gives too low height values. No error fields are given on figs. 2 e and i in order not to overload these figures. The positions of the centres for extreme values of the errors are, however, approximately the same as the ones indicated on the other forecast charts. Especially, this is the case if we compare forecasts B and C.

On fig. 2 g and k are given the observed 24h and 48h changes, respectively. From the error field the following conclusions may be drawn.

The most serious errors are those connected with (1) the trough from Iceland to the central part of the Mediterranean; (2) the low over the Atlantic and (3) the strong anticyclogenesis in the upper left corner of the chart. The errors (1) is brought about by the fact that this trough maintained its position under filling, while the forecast moved it to the northeast keeping its central value unchanged. The errors (2) are obviously connected with a baroclinic development of a low east of Newfoundland. Finally the errors (3) are caused by an intense fictitious anticyclogenesis over the Alaska region and the area south thereof. This must be due to the boundary error effect as pointed out by BOLIN (1955). Keeping the boundary values constant in such an area with strong cyclonic activity means a serious drawback to the value of the forecast. The numerical value of the error in this area exceeds 400 gdm even for the 24h forecasts.

A striking feature of the error fields in fig. 2 d and h is the large increase of the numerical value of some of the extreme areas. Over Canada a change from −50 gdm to −250 gdm was observed. The maximum value of −200 gdm over Central Europe in fig. 2 d increased, numerically speaking, to −340 gdm over Scandinavia in fig. 2 h.

In spite of the fact that the numerical values of the error sometimes increase or decrease radically, a certain conservatism in the error field can be seen, if we compare the field for a 24h and 48h forecast. Comparing consecutive 24h forecasts and their corresponding error field this is more obvious. When using numerical forecasts on an operational basis this fact must be of some value. PETTERSSEN (1956)

Table IV. Some verification parameters computed for different 500 mb 24h forecasts valid for 0300 GMT 8 November 1949. Heights are given in geodynamic meters and wind speeds in m/s.

Analysis	A	B	C	B[1]	B[11]
$\bar{y}$	−22	−6	−5	−7	−6
σ_y	77 (69)	66 (70)	62 (73)	66 (69)	69 (73)
$\overline{\lvert y \rvert}$	63	54	51	52	56
ε_0	64	52	58	49	50
r_{xy}	0.67 (0.68)	0.74 (0.73)	0.68 (0.67)	0.77 (0.75)	0.77 (0.78)
δ_e	11.4	9.4	10.5	9.1	9.2
δ_p	12.3 (10.7)	10.2 (11.2)	9.1 (11.5)	9.9 (10.9)	10.1 (11.1)
$\bar{d}_p$	10.4 (9.3)	9.0 (9.9)	7.9 (9.6)	8.8 (9.6)	9.0 (9.8)
$\bar{d}_e$	9.0	7.8	8.6	7.7	7.8
(d_e)max	38.2	28.5	36.1	27.5	27.5
$r_{d_e d_p}$	0.40 (0.44)	0.56 (0.49)	0.55 (0.37)	0.54 (0.48)	0.53 (0.48)

Table V. Some verification parameters computed for different 500 mb 48h forecasts valid for 0300 GMT 9 November 1949. Heights are given in geodynamic meters and wind speeds in m/s.

Analysis	A	B	C	B[1]
$\bar{y}$	−48	−2	6	38
σ_y	146 (137)	124 (129)	124 (132)	112 (106)
$\overline{\lvert y \rvert}$	125	99	101	95
ε_0	133	92	87	88
r_{xy}	0.66 (0.61)	0.72 (0.70)	0.74 (0.77)	0.72 (0.69)
δ_e	15.8	13.7	12.6	12.7
δ_p	16.8 (15.1)	15.5 (16.9)	14.1 (15.8)	15.5 (16.7)
$\bar{d}_p$	15.0 (13.4)	14.1 (13.2)	12.7 (13.9)	14.0 (13.1)
$\bar{d}_e$	14.2	12.2	11.4	11.4
(d_e)max	31.4	29.5	27.0	28.0
$r_{d_e d_p}$	0.23 (0.11)	0.31 (0.38)	0.39 (0.49)	0.39 (0.32)

has reported on an experiment carried out at the research centre in Chicago. The numerical forecasts were scrutinized by experienced forecasters using their general knowledge of the behaviour of the atmosphere from a barotropic point of view as well as statistics of the misbehaviour of the barotropic model published among others by GATES ET AL. (1956). On top of this a systematic use of the quasi-conservatism of the error fields might be of some value. It would lead too far, however, to enter on a detailed discussion on this subject in this paper.

In tables IV and V some verification figures are given. These values ought to be compared to the corresponding values in table VI. Subscripts x and y stand for observed and forecast changes, respectively.

The same symbols are used as in paper I (p. 332).

The variations of the numerical values in table IV are mostly between 10 and 30 per cent of the mean values. In two cases the differences are quite large: the value of $\bar{y}$ varies between −5 and −22 gdm and the value of r_{d_e, d_p} between 0.40 and 0.56. Comparing the

Table VI. Some observed quantities for the 24h (48h) period ending at 0300 GMT 8 (9) November 1949. Heights are given in geodynamic meters and wind speeds in m/s.

	24h			48h		
Analysis	A	B	C	A	B	C
$\bar{x}$	2	−3	−3	23	19	18
σ_x	69	74	78	117	117	112
$\overline{\lvert x \rvert}$	53	56	59	90	90	86
δ_0	10.8	11.8	12.4	16.9	16.4	15.4
d_0	9.1	9.9	10.2	14.4	14.1	13.3
(d_0)max	32.5	38.7	39.9	39.6	38.4	33.8

values of $\bar{x}$ in table III we find that the variation in $\bar{y}$ is much larger than in $\bar{x}$.

The percentage variations in table V are for most quantities larger than the corresponding values in table IV.

If we now compare tables IV and V with table II in paper I (p. 333) we notice that the variations given in this paper are larger and in some cases much larger than the earlier ones. This is natural as we now deal with differences in forecasts based on different analyses and in the earlier case with differences caused by different verification analyses. The effect is, however, counteracted by the fact that in paper I 26 (29) analyses were discussed while in this paragraph we are only discussing three different forecasts.

As was already stated in the introduction the situation chosen for this and the earlier study is a rather simple one from the analyst's point of view. It would be rather difficult to find a case that were definitely simpler to analyse if we regard the rather large area covered. For that reason it is the author's opinion that the values given in this paper and in paper I represent near minimum values.

When combining the x- and y-values in order to get the numerical quantities in table IV and V the x-values were taken as the differences between analyses A, B and C, respectively, and the verification analyses for the 8th and 9th of November 1949. It is possible to combine, say, an x-value taken as the difference between the verification analysis and analysis A and combine it with a y-value corresponding to analysis B. This was done for all possible combinations between x- and y-values corresponding to analyses A, B and C. The values that showed the largest numerical deviation from the ones calculated with the aid of the natural combinations are given within parantheses in table IV and V. Thus, for each forecast we get three different sets of verification quantities. If we compare the values corresponding to the same forecast we have almost the same combination of charts as was discussed in paper I: fixed values of the forecast changes correlated with values of observed changes varying with differences in the analysis of either the initial or the verification chart. In the earlier case the verification chart varied and this time the initial chart is the variable one. The values within parantheses deviate in some cases rather much from the already discussed values. In table V we get a value of r_{xy} for analysis A, that is 0.61 instead of 0.66. The values of $\bar{d}_p$ in the same table and the same column are 13.4 and 15.0 m/s, respectively, and those of $r_{d_0,\ d_p}$ 0.11 and 0.23, respectively.

It is natural to expect that the deviations due to different forecasts should represent larger values than those due to differences in verification analyses or in the initial analyses as the values are calculated in this special case. As can be seen in tables IV and V this is the rule except in a few places.

Let us now return to table I and compare the standard deviation of the difference between analyses A, B and C, respectively, with the same quantities for the corresponding forecasts. The largest increase is observed for the analysis pair A – B, for which the d-value increased from 26 to 54 gdm. For the pair B – C the increase is somewhat less, from 27 to 41 gdm. We notice that the d-values are approximately the same for all combinations of 24h forecasts. It is remarkable that the pair A – C shows a constant d-value during 48 hours.

2. *Comparison between two forecasts based on two different analyses*

As can be seen from fig. 2 there are some differences between analyses A and B^1. The largest deviations are observed over northeast Greenland and the area around the North Pole, over the Alps and northern Italy and the region south of the Azores. Minor differences are found in the upper part of the area given in fig. 2. Very much alike are the position of the low over northeast Canada and of the trough from Iceland to the Mediterranean.

From table IV we get the resulting verification figures. The correlation coefficient (r_{xy}) increased to the highest value in the table (0.77) and all the wind verification figures were lower for the B^1-case. The largest percentage drop was observed for the $\bar{y}$-value(– 22 and – 7 gdm, respectively), and the second to the largest for the ε_0-value. The $r_{d_0,\ d_p}$-value increased from 0.40 to 0.54. On the whole one must conclude, however, that the variation of the verification figures does not increase noteworthy when we include analysis B^1 and the corresponding 24h forecast in table IV. This is of course due to the fact that the difference between the forecasts based on analyses B and B^1, respectively, are rather small. This fact will be subject to a somewhat more detailed discussion in the next paragraph.

For the 48h forecasts the differences are larger than for the 24h ones, but the deviations are by no means great. A large difference is observed, however, in the δ_e-value, this "wind error" being 15.8 and 12.7 m/s, respectively. The largest difference is that of the $\bar{y}$-value, −48 and +38 gdm, respectively. If we disregard this difference the following conclusion can be given from an inspection of the parts of tables IV and V discussed so far: *in this case the inclusion of a new analysis with a different boundary region did not give rise to larger differences than were already observed using analyses with identical boundary analysis and different inner region analyses.*

The above conclusions are the same if we look at table I. The *d*-values show only small differences if we compare the analysis pair $A - B^1$ instead of $A - B$.

A visual inspection of the 24h forecast charts of fig. 2 gives the result that both sets of forecasts fail to predict the right position of the Mediterranean trough. Due to the extreme vorticity values combined with large wind velocities given by analysis A over Italy, the forecast based on this chart moved the trough more to the northeast than did the corresponding forecast based on analysis B^1 and at the same time the trough became sharper. It is, however, interesting to note that a new trough is situated over the Central part of the Mediterranean.

The low over northeastern Canada has the same position on the two forecast charts and the same is true for the ridge from the North Sea to Spitzbergen. Apart from the trough over Central Europe the two forecast charts ought not to result in two substantially different general forecasts for the verification area, i.e. the translation of forecast upper stream patterns into weather ought to be rather similar. In other words: if we disregard the trough over Central Europe there is no significant operational difference between the two forecasts.

A comparison between the 48h forecast charts shows that the deviations are larger than was the case for the 24h forecasts. It is beyond all doubt that for some areas a translation into weather of the 500 mb stream pattern would result in significantly different forecasts. This is true over the Baltic and adjacent areas, over the Central part of the Atlantic Ocean and the Mediterranean and finally over portions of the North-American continent. Subjectively speaking one could say that there exists an operational difference between the 48h forecast charts.

Best (1956) has given some examples on deviations between forecasts based on different analyses of (practically) the same observation material.

His conclusion was that "the prognostic differences do not appear to be of major importance on the 24h forecasts. However, for forecast periods of 48h and 72h, the prognostic differences seem large enough to be operationally significant."

A very large deviation was reported by Newton (1954) who by reanalyzing a 500 mb chart over the area southwest of Ireland got an increase of r_{xy} from 0.06 to 0.41. In his case mean values of computed instantaneous tendencies twelve hours apart were compared with twelve hour observed changes.

3. *Comparison between forecasts based on two analyses with identical inner region but with different boundary regions.*

As already stated in the foregoing paragraph the difference between forecasts based on analyses B and B^1 did not differ too much from each other. Fig. 2 indicates that as far as the 24h forecasts are concerned the only noteworthy difference within the verification area is to be found over westernmost Atlantic. On the 48h forecast charts some differences are noteworthy over the North-American continent. The low over eastern Canada has deepened somewhat on the B-forecast while the B^1-forecast shows a slight filling. The low off the American westcoast on the initial charts is situated west of the Rocky Mountains on one chart and over or just east of the divide on the other.

In the boundary area in the upper left corner of the chart the boundary error are very different on the two charts.

The conclusion is that for some areas the two 48h forecasts may be regarded as slightly operationally different.

An inspection of table IV gives the result that analysis B^1 gave a slightly better 24h forecast than did analysis B. Practically all verification parameters show a decrease in their numerical value but the decrease is small, indeed. The correlation coefficient rose from 0.74 to 0.77. The differences given in table IV can hardly be said to be significant.

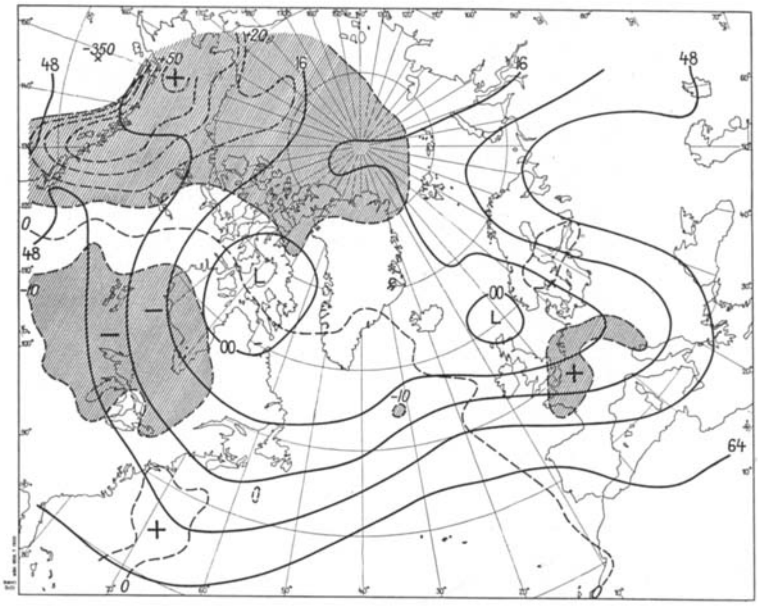

Fig. 3. 500 mb 24h barotropic forecast valid for 0300 GMT 8 November 1949 (cf. fig. 2e, solid lines). Dashed lines give the difference between the forecast and an "erroneous" one (see paragraph 4) with values *numerically* larger than 10 gdm indicated by hatching.

The differences for the 48h forecasts are larger for some quantities. This is especially true for the $\bar{y}$-value and also to some degree for the δ_e-value and $\bar{d}_e$-value.

4. *Discussion of the influence of an isolated erroneous grid value on the forecast*

During the punching of the initial data for analysis B^1 in order to get it into a form suitable for the BESK computer, an error in the punching equipment gave a wrong grid point value for the point encircled in fig. 1. The grid point is situated over the Gulf of Alaska. Instead of the correct value (5)280 gdm the machine punched (5)080 gdm. This error was not traced because in the first print-out the value 280 was given.

This large point error seemed to have a peculiar influence on the computations. The 24h forecast was received without trouble, but when plotted and analyzed it was discovered that in the region of the wrong initial grid value a very peculiar pattern was obtained. During the continued calculation the number of iterations ran to rather high values and after 11 timesteps the calculations were stopped, i.e. after $24h + 11 \times 1.2 \simeq 37h$. The 37h forecast contained some very odd values south of Alaska and it was not possible to analyze that area without getting enormous gradients and a couple of small distinct lows and highs.

The fact that the wrong initial grid point was situated quite a long distance from the verification area gave the result that the verification figures for the 24h forecast based on the "wrong" analysis (called B^{11} in the following) did not differ much from those of the B^1-forecast. In table IV are given the verification figures and we can see that the differences are very slight.

It is interesting to study the distribution o the difference between the B^1- and B^{11}-forecasts. These differences are given in fig. 3. Within the verification area the differences for large regions are less than 5 gdm, numerically speaking. The mean value of the absolute value of the difference calculated for the verification area was 5.7 gdm. As can be seen from the figure the influence of the error over the inner region is very slight. The computation did, however, break down, the number of iterations increasing from $2-4$

during the first 24 hours to 26 just before the calculations were stopped.

5. Differences between the value of some parameters calculated from a set of analyses.

In the forecast scheme used in connection with the forecasts discussed in this paper the following equations are used

$$\xi = \nabla^2 \phi \qquad (1)$$

$$\eta = \frac{m^2}{f} \xi + f \qquad (2)$$

$$\frac{\partial \xi}{\partial t} = \frac{\partial \eta}{\partial x} \cdot \frac{\partial \phi}{\partial y} - \frac{\partial \eta}{\partial y} \cdot \frac{\partial \phi}{\partial x} = J(\eta, \phi) \qquad (3)$$

where ϕ is the geopotential of the 500 mb surface, $\xi = fm^{-2} \zeta$ (ζ is the relative vorticity), η the absolute vorticity, m the mapping factor $\left(m = \frac{1 + \sin 50^\circ}{1 + \sin \phi} \text{ in this case}\right)$ and f the Coriolis parameter.

During the computation the quantity

$$\nabla^2 \phi_{i,j} = \phi_{i,j+1} + \phi_{i,j-1} + \phi_{i+1,j} + \phi_{i-1,j} - 4\phi_{i,j} \qquad (4)$$

is computed. Furthermore the quantity

$$J_{i,j}(\eta, \phi) = (\eta_{i+1,j} - \eta_{i-1,j})(\phi_{i,j+1} - \phi_{i,j-1}) - (\eta_{i,j+1} - \eta_{i,j-1})(\phi_{i+1,j} - \phi_{i-1,j}) \qquad (5)$$

is calculated (scale factors is also applied in the two cases but they are disregarded here).

The differences observed between the forecasts as discussed in the paragraphs 1 – 3 must be due to differences in the initial distribution of the geopotential of the 500 mb surface. As they occur in the initial charts discussed in this paper, they are entirely due to differences between the analyses caused by the personal factor in upper air analysis. It might be of interest to calculate some parameters from the 26 different analyses referred to earlier. For a small area centered over Central Europe (see fig. 1) a calculation was made of the standard deviation (s) of ζ and $\nabla^2 \phi_{i,j}$ and of $J(\eta, \phi)$ and $J_{i,j}(\eta, \phi)$. The first two quantities were computed for all 70 grid points within the indicated area and the other two for 23 grid points evenly spaced over the area.

A visual inspection of charts containing the distribution of the s-values for the four quantities (not shown in this paper) defined above gives the following result. The s-value for ζ and $\nabla^2 \phi_{i,j}$ show rather confused patterns and it is not possible to notice any connection between these and the isohypse pattern or the pattern of the isotachs of the geostrophic wind. The highest values were found at one grid point over Poland and the second to the largest over Italy. Minimum values occurred over Scotland and in a narrow band from northern Ireland to Central Germany.

As for the s-values for $J_{i,j}(\eta, \phi)$ and $J(\eta, \phi)$ they were much more regularly distributed. The highest values was observed in the northwesterly current from the Bay of Biscay to Sardinia while the minimum values occurred in the trough from the North Sea to the Alps.

Table VII. The standard deviation (s) of some parameters in equations 1—5.

	$\bar{s}$	s_{max}	s_{min}	units
$\nabla^2\phi_{i,j}$	28.4	49.1	13.6	gdm
$J_{i,j}(\eta,\phi)$	$561 \cdot 10^{-4}$	$1110 \cdot 10^{-4}$	$132 \cdot 10^{-4}$	MTS
ζ, η	$3.2 \cdot 10^{-5}$	$5.1 \cdot 10^{-5}$	$1.1 \cdot 10^{-5}$	MTS
$J(\eta,\phi)$	$16.3 \cdot 10^{-14}$	$32.6 \cdot 10^{-14}$	$3.4 \cdot 10^{-14}$	MTS

In table VII are given mean values of s over the 70 (23) grid points together with the extreme grid point values observed within the area.

Taking the $\bar{s}$-value of 28.4 gdm for $\nabla^2 \phi_{i,j}$ from table VII, it might be of interest to compare it to the value of the standard deviation of the height of the 500 mb (σ_h) as given in paper I. The value of σ_h represents the variations due to the personal factor in analysis. Its mean value over the area considered in this paragraph was 13.1 gdm. Assuming that the value at one grid point is independent of the value at nearby grid points, we get the value $\sqrt{20} \cdot 13.1 = 58.7$ gdm for the value of s for $\nabla^2 \phi_{i,j}$. The actual value in table VII is 28.4 gdm, the difference being due to the correlation between the value of σ_h at adjacent grid points.

The mean value of s for the vorticity is $3.2 \cdot 10^{-5}$ sec^{-1} and this value ought to be compared to the mean values of the relative and absolute vorticity for the investigated area. These mean values are $3.2 \cdot 10^{-5}$ and $14.0 \cdot 10^{-5}$ sec^{-1}, respectively.

The mean value of s for $J_{i,j}$ (η, ϕ) ought to be compared to the mean deviation of the mean value of the same quantity calculated for the 23 grid points and from the 26 analyses, this value being $96 \cdot 10^{-4}$ MTS. The mean value for the whole area is $4 \cdot 10^{-4}$ MTS, while the mean value of the range at each grid point is $2{,}270 \cdot 10^{-4}$ MTS.

Considering equation (3) and the mean value of s for J (η, ϕ) given in table VII, we notice that the corresponding value of $\triangle\xi$ is equal to $5.9 \cdot 10^{-10}$ MTS, when the time step is one hour.[1]

Thus, the value of $\bar{s}$ for J (η, ϕ) corresponds to a value of $\triangle\xi$ (for a time step of one hour) that is 1/6 of the value of ξ itself as the mean value and the mean deviation of ξ for the area under consideration is $35.7 \cdot 10^{-10}$ and $40.3 \cdot 10^{-10}$ MTS, respectively.

The first conclusion one draws when faced with the values in table VII may be that forecasts based on these different analyses ought to be quite different. As has been pointed out in paragraph 1 through 3, this is not the case. The explanation for this apparent discrepancy is given by THOMPSON in an article published in 1954. In his paper Thompson shows that the solution of the vorticity equation for quasi-geostrophic flow can be given in terms of the first derivatives of the height of the pressure surface used. The errors in computing second and third order derivates are cancelled out in the process of solving the vorticity equation. Thompson emphasizes that errors in reported observations are non-systematic and therefore the percentage errors in the solution of the vorticity equation are generally much less than the percentage errors in the computed vorticity advection at individual points. In the case studied here, however, the differences in the analyses are to some extent systematic as they depend largely on the character of the network of upper air observing stations. Furthermore, the reported deviations are mean values for an area of approximately 2,700 × 1,800 km and do not represent errors at individual points.

[1] The calculations are actually performed in such a way that $\triangle\xi = \xi^t - \xi^{t-2\triangle t}$ and the corresponding Jacobian is computed for $(t - \triangle t)$. For the first two time steps it is not possible to use centered differences and then $\triangle\xi = \xi^{\triangle t/2} - \xi^0$ with the corresponding Jacobian for $t = 0$ and $\triangle\xi = \xi^{\triangle t} - \xi^0$ together with $J(\eta^{\triangle t/2}, \phi^{\triangle t/2})$, respectively.

REFERENCES

BERGGREN, R., 1957: On the accuracy of 500 mb analysis with special reference to numerical forecasting. Tellus, 9, No. 3, pp. 323—340.

BERGTHORSON, P., and DÖÖS, B., 1955: Numerical weather map analysis. Tellus, 7, No 3, pp. 329—340.

BEST, W. H., 1956: Differences in numerical prognoses resulting from differences in analyses. Tellus, 8, No. 3, pp. 351—356.

BOLIN, B., 1955: Numerical forecasting with the barotropic model. Tellus, 7, No. 1, pp. 27—49.

CRESSMAN, G. P., and GILCHRIST, 1954: An experiment in objective analysis. Tellus, 6. No. 4, pp. 310—318.

DÖÖS, B., and EATON, Mc., 1957: Upper-air analysis over ocean areas. Tellus, 9, No. 2, pp. 184—194.

GATES, W. L., POCINSKI, L. S., and JENKINS, C. F., 1956: Results of numerical forecasting with the barotropic and thermotropic atmospheric models. Geophys. Res. Pap., No. 46.

NEWTON, C. W., 1954: Analysis and data problems in relation to numerical prediction. Bull. Am. Met. Soc., 35, No. 7, pp. 287—294.

PETTERSSEN, S. ET AL., 1957: An experiment in prognostication (Studies in weather analysis and forecasting, Part G) Final Rep. Contract AF 19 (604)—1293. Dept. Met., Univ. of Chicago, 32 pp.

Staff Members, Inst. of Met., Univ. of Stockholm, 1954: Results of forecasting with the barotropic model on an electronic computer (BESK), Tellus, 6, No. 2, pp. 139—149.

THOMPSON, P. D., 1954: A note on the integration of the vorticity equation for quasi-geostrophic flow. Tellus, 6, No. 6, p. 319—325.